Methylation of benzene by methanol: Single-site kinetics over H-ZSM-5 and H-beta zeolite catalysts

Jeroen Van der Mynsbrugge[1], Melina Visur[2], Unni Olsbye[2], Pablo Beato[3], Morten Bjørgen[4], Veronique Van Speybroeck[1,*], Stian Svelle[2,*]

[1] Center for Molecular Modeling (CMM), Ghent University, Technologiepark 903, 9052 Zwijnaarde, Belgium and QCMM Alliance, Ghent-Brussels, Belgium

[2] inGap Center of Research Based Innovation, Department of Chemistry, University of Oslo, P. O. Box 1033 Blindern, N-0315, Oslo, Norway

[3] Haldor Topsøe, Nymøllevej 55, DK-2800 Kgs. Lyngby, Denmark

[4] Department of Chemistry, Norwegian University of Science and Technology, Høgskoleringen 5, 7491 Trondheim, Norway

[*] corresponding authors:

Stian Svelle
e-mail: stian.svelle@kjemi.uio.no
Phone: +47 22 85 54 54; Fax: +47 22 85 54 41

Veronique Van Speybroeck
e-mail: veronique.vanspeybroeck@ugent.be
Phone: +32 9 264 65 58; Fax: +32 9 264 66 97

ABSTRACT

Benzene methylation by methanol is studied on acidic zeolites H-ZSM-5 (MFI) and H-beta (BEA) to investigate the influence of the catalyst topology on the reaction rate. Experimental kinetic measurements at 350 °C using extremely high feed rates to suppress side reactions show that methylation occurs considerably faster on H-ZSM-5 than on H-beta. Theoretical rate constants, obtained from first-principles simulations on extended zeolite clusters, reproduce a higher methylation rate on H-ZSM-5 and provide additional insight into the various molecular effects that contribute to the overall differences between the two catalysts. The calculations indicate this higher methylation rate is primarily due to an optimal confinement of the reacting species in the medium pore material. Co-adsorption of methanol and benzene is energetically favored in H-ZSM-5 compared with H-beta, to the extent that the stabilizing host-guest interactions outweigh the greater entropy loss upon benzene adsorption in H-ZSM-5 vs. in H-beta.

KEYWORDS

zeolite, H-ZSM-5, H-beta, methanol, benzene, methylation, kinetics, first principles, DFT-D, methanol to hydrocarbons

1. INTRODUCTION

Methylation reactions catalyzed by acidic zeolites are highly important in several transformation processes of hydrocarbons [1]. Methylations were also shown to be crucial steps in the zeolite-catalyzed conversion of methanol to hydrocarbons (MTH), which was first discovered in 1976 and has since been developed into a number of commercial technologies, for example, methanol-to-gasoline (MTG) [2], methanol-to-propylene (MTP) [3] and methanol-to-olefins (MTO) [4]. At present, MTO is one of the most prominent alternatives to crude-oil cracking for the production of light olefins such as ethene and propene [5]. The exact mechanism underlying the conversion process has been debated for decades, but currently there is a consensus on an indirect mechanism in which methanol is converted to light olefins via repeated methylation and/or cracking reactions of a pool of hydrocarbons present inside the zeolite pores [6-13]. In every catalytic cycle proposed to date to explain olefin formation, methylations were found to be key reaction steps [14-16]. For these reasons methylations have received a lot of attention in several recent studies, in which they were examined from both an experimental and a theoretical angle [17-21].

Most zeolite-catalyzed processes are the result of a complex mechanism, consisting of a large number of both consecutive and competing elementary steps. Obtaining detailed information about any individual reaction is therefore non-trivial from an experimental point of view, as the rate of a single reaction is not easily monitored. Svelle et al. first accomplished this for specific methylation reactions of alkenes by methanol on zeolite H-ZSM-5 [17, 18], and more recently Hill et al. performed an experimental study on the kinetics of alkene methylation by dimethyl ether on zeolites H-ZSM-5, H-beta, H-ferrierite, and H-mordenite [22], but in general experimental kinetic measurements of isolated zeolite-catalyzed reactions are rarely reported.

Theoretical methods offer the advantage that they innately allow isolating a single reaction step to study its various molecular aspects in detail. However, these methods have only recently matured to a level where energy barriers and reaction rates can be determined that are directly comparable with experimental data [19, 20]. Further development of theoretical methods depends on the availability of accurate experimental data to benchmark the calculations, such that a combined approach offers the best prospects for an improved understanding of these elementary steps.

In this article, we study the methylation of benzene by methanol in two zeolite catalysts with different topologies: MFI-structured H-ZSM-5 and BEA-structured H-beta. Experimental and theoretical methods are combined to determine the influence of topological variations in the catalyst on the methylation rate. Both frameworks consist of intersecting channels that are sufficiently spacious to allow direct feeding of benzene, and both catalysts have been the subject of previous research in the field of MTH-conversion. H-ZSM-5 is among the most widely used catalysts in industrial applications, and is also the archetypal catalyst in methanol to hydrocarbons conversion. This catalyst has been studied extensively, by experimental as well as theoretical research groups. H-beta also shows MTH-activity, but is more of academic interest. The large-pore structure allows direct feeding of even larger species than in H-ZSM-5, making H-beta an ideal candidate for the study of mechanistic aspects, the activity of larger hydrocarbon pool species and the formation of coke precursors [14, 23-25]. However, because of its large-pore structure, MTH-conversion in H-beta results in a product stream consisting predominantly of larger components such as hexamethylbenzene. These products are already too heavy to be used in gasoline, for which the C_{10}-content should be limited. H-beta furthermore suffers from rapid deactivation through coke formation, rendering this zeolite unsuitable for industrial MTH applications.

As far as the mechanism of the zeolite-catalyzed methylation reaction is concerned, two different proposals have been advocated in literature: a stepwise route that involves a surface-bound methoxy group intermediate, and a concerted mechanism in which physisorbed methanol directly interacts with the species to be methylated [22, 26, 27]. While spectroscopic evidence for the existence of surface-bound methoxy groups has been presented, and the fundamental viability of a stepwise mechanism has been verified, experimental kinetic measurements are readily explained by the concerted pathway [26, 28]. For this reason, the latter mechanism will be presumed in the current article. Nevertheless, no definitive conclusion regarding the prevailing pathway is warranted at this point; a full discussion of this issue has been given elsewhere [26].

A general overview of the methylation of benzene by methanol in an acidic zeolite catalyst is represented in Figure 1. Conceptually, for methylation to occur, methanol should be adsorbed at the Brønsted acid sites. Methanol will then react with a benzene molecule loosely adsorbed in the vicinity of the methanol molecule. Experimental barriers and reaction rates are therefore always referred to the state in which methanol is adsorbed and benzene is still in the gas phase. Kinetic parameters corresponding to this viewpoint are called “apparent”, to distinguish them from the “intrinsic” kinetics associated with the actual methylation step, through re-organization of both reactants adsorbed at a specific active site. The methylation products encountered after the transition state are a toluenium ion and water. The toluenium ion can be assumed to deprotonate rapidly, yielding toluene and regenerating the Brønsted functionality of the catalyst.

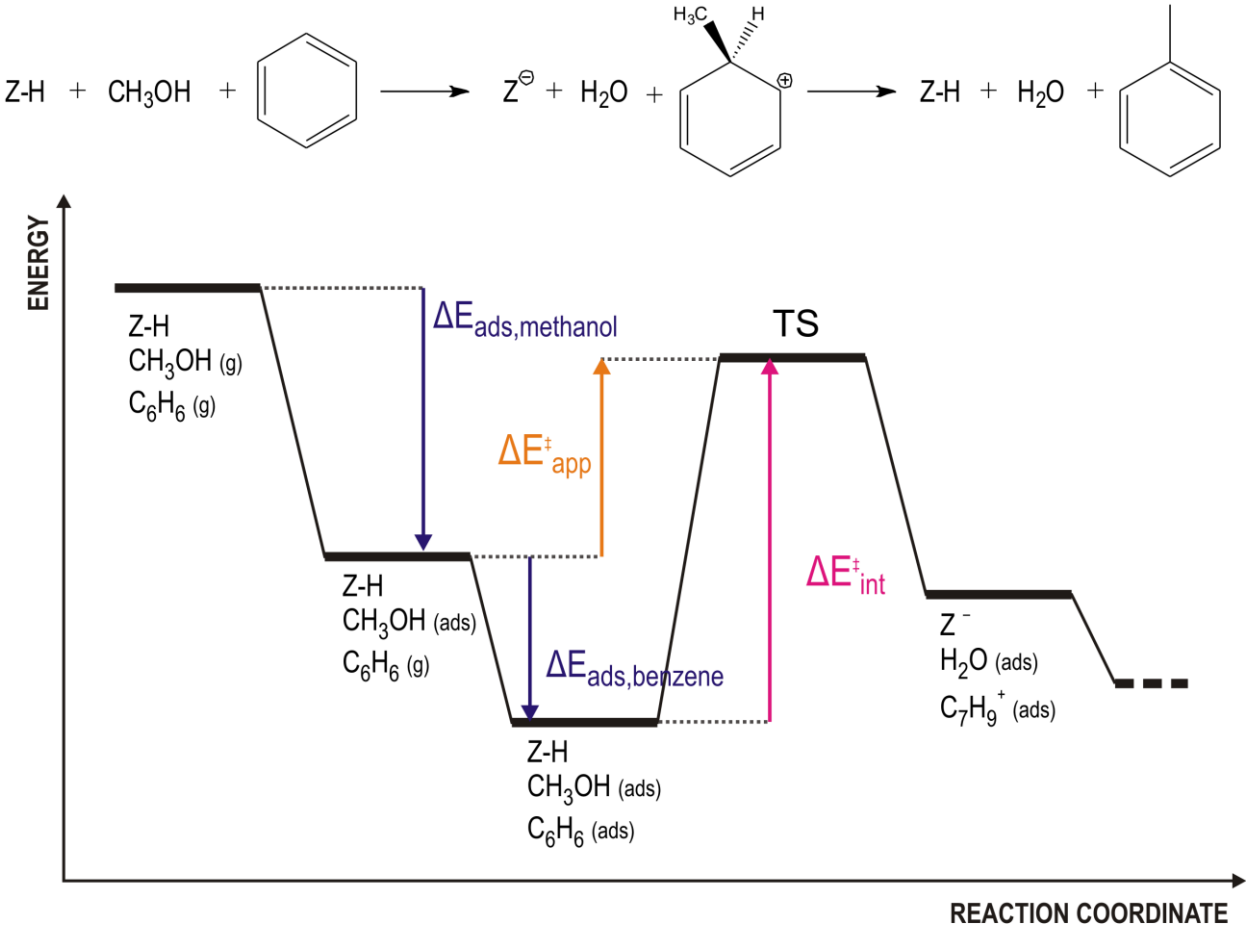

Figure 1. Schematic energy profile for the zeolite-catalyzed methylation of benzene by methanol.

2. METHODS

2.1. EXPERIMENTAL METHODS

2.1.1. CATALYSTS AND CATALYST CHARACTERIZATION

Two catalysts were employed in this study, an H-ZSM-5 sample supplied by Süd Chemie and an H-beta sample synthesized in-house. Notably, this is the same H-ZSM-5 catalyst as employed in our previous studies of the methylation of alkenes [17, 18]. These catalysts were selected due to similarities with respect to crystal size and acid site density.

The H-beta catalyst was synthesized based on published procedures [29]. Degussa Aerosil 380 (SiO_2) was homogenized into a 20 % aqueous solution of the tetraethylammoniumhydroxide template (TEAOH). Subsequently, an aqueous solution of $Al(NO_3)_3$ was added and the mixture thus formed homogenized by vigorous stirring for 10 min. The molar composition of the gel was 100 SiO_2 : 0.26 Al_2O_3 : 53.8 TEAOH : 1550 H_2O. The gel was transferred to a Teflon-lined steel autoclave and crystallized for 60 h at 140 °C. The solid product thus obtained was washed/centrifuged with ion-exchanged water three times and dried at 110 °C for 12 h. The template was removed by slow heating to 450 °C in a flow of N_2 and O_2 (equal partial pressures) followed by stepwise heating to 550 °C in a pure O_2 flow. The final temperature was maintained for 12 h. The final, protonic material was obtained by ion exchange using 1 M NH_4NO_3 for 3 × 2 h at 70 °C, followed by calcination in static air at 550 °C for 3 h.

The catalysts were characterized using a variety of methods, paying particular attention to a quantitative and qualitative evaluation of the acidic properties. Phase purity was investigated with capillary X-ray diffraction (XRD) employing a Siemens-Bruker D5000 diffractometer

using Cu Kα1 radiation. Particle size was determined using transmission electron microscopy (TEM; JEOL JEM 2000FX with an acceleration voltage of 100 kV) and scanning electron microscopy (SEM; FEI Quanta 200 FEG-ESEM). BET surface areas were assessed from N_2 physisorption on a Belsorp-mini II instrument at -196 °C. The chemical environment of Al was probed using ^{27}Al MAS-NMR (Bruker Avance 200 DMX). Elemental analysis was performed using an HR-ICP-MS Element 2 instrument from Thermo Scientific. The samples were dissolved in hydrofluoric acid. The densities of acid sites were calculated using temperature-programmed desorption (TPD), assuming that one ammonia molecule corresponds to one Al substitution. A qualitative evaluation of acid strength was carried out by following the adsorption of CO at low temperature with Fourier transform infrared spectroscopy (FTIR). Transmission FTIR spectra were recorded on a Bruker Vertex 80 spectrometer equipped with an MCT detector. Dehydrated, self-supporting wafers were cooled to -196 °C, and CO was adsorbed until saturation. Subsequently, CO was allowed to desorb in small steps and FTIR spectra were recorded.

2.1.2. KINETIC MEASUREMENTS

A description of the experimental setup has been given in a previous paper [17, 18]. Briefly, all kinetic measurements were carried out at atmospheric total pressure using a 3 mm inner diameter fixed bed reactor. In most experiments, 2.5 mg catalyst (particle size 250 - 420 µm) was used, in order to achieve the very high feed rates required to study the kinetics of primary reaction steps. ^{13}C methanol (Cambridge Isotope Laboratories; chemical purity >99 %; isotopic purity >99 %) and ^{12}C benzene (Sigma Aldrich, purity >99.5 %) were introduced by passing parts of the He carrier gas flow through saturation evaporators maintained at controlled temperatures to regulate the partial pressures. The typical gas flow through the reactor was 75

N mL min^{-1}, with partial pressures of methanol and benzene of 37 and 17 mbar, respectively. The resulting feed rate was WHSV = 195 $g_{feed}g_{catalyst}^{-1}h^{-1}$, corresponding to a contact time (CT = $WHSV^{-1}$) of 0.0051 h. The total gas flow and the partial pressure of each reactant were varied in three separate measurements series. The reaction temperature was measured using a thermocouple (0.5 mm diameter) in direct contact with the catalyst. The typical reaction temperature was 350 °C, but the temperature was varied between 250 and 400 °C to determine the Arrhenius activation energies. Although the catalyst samples were fairly resistant toward deactivation, a slight loss of activity was observed. This was corrected for using previously described procedures [6, 8]. A primary concern has been to study the catalytic system at low conversion (i.e., high feed rates) to prevent side reactions, while still operating at a realistic reaction temperature and catalyst acid site density.

The conversion and product distribution were determined using an on-line HP6890 GC-FID equipped with a Supelco SPB-5 column (60 m × 0.53 mm × 3 μm). The isotopic composition of the major products was determined from analyses carried out on a HP 6890 GC- MS unit, using a J&W GS-GasPro column (60 m × 0.32 mm). The procedure for calculating the isotope distributions from the mass spectra has been outlined previously [7].

2.2. COMPUTATIONAL METHODS

The methylation reaction was modeled from first principles to further rationalize the experimentally observed differences between the two catalysts. In this article, extended cluster models consisting of 46 and 52 T-atoms for H-ZSM-5 and H-beta, respectively, were used (represented in Figure 2) [14-16]. This approach has previously proven a reliable and computationally efficient method to predict rate coefficients and reaction barriers that are very

close to experimental kinetic data [14, 20]. In contrast to periodic calculations, in which the entire unit cell is taken into account, cluster calculations only consider a fragment of the crystallographic structure. However, an extended cluster, provided it is large enough to account for the distinguishing topological features of the catalyst, was shown to be able to describe all relevant confinement effects as well [20, 30]. The cluster approach has some advantages that are particularly useful for deriving first-principle kinetics; the localization of transition states is considerably simplified, and the vibrational analysis is more straightforward [20].

H-ZSM-5 (MFI) consists of intersecting straight and zigzag channels that range from 0.51 to 0.56 nm in diameter, resulting in medium-sized pores, while H-beta (BEA) has slightly larger intersecting straight channels, with a diameter of 0.55 - 0.67 nm (see Figure 2) [31]. In both catalysts, an active site was positioned at the channel intersection, as these locations offer maximal available space in each topology and result in minimal restrictions, even when bulky intermediates are involved. Additionally, previous studies on the adsorption of benzene and its derivatives in silicalite (MFI) have shown that these molecules adsorb preferentially at the channel intersections [32].

In the MFI-topology the location of the aluminum defect corresponds to the T12 crystallographic position [33]. A thorough examination of all possible active sites is clearly beyond the scope of this study. This is furthermore not straightforward, as it was recently shown for H-ZSM-5 that the actual aluminum distribution in a zeolite material does not only depend on thermodynamic stability, but rather on the conditions applied during the synthesis of the catalyst [34-36].

Dangling bonds on the boundary of the cluster fragments were saturated with hydrogen atoms, which are constrained in space to avoid unrealistic distortions of the model during geometry optimizations. Stationary points were localized using the two-level method ONIOM(B3LYP/6-31+G(d):MNDO) in which a central 8T cluster and the guest molecules are treated at the higher level of theory, in accord with our previous studies on H-ZSM-5 [15, 16, 20]. For the beta catalyst the convergence of the transition state geometry with respect to the high level size was confirmed in the current study. Extension toward 10T high level did not result in further geometry changes. The nature of the stationary points was verified by a normal mode analysis, resulting in only real frequencies for the minima, and a single imaginary frequency for the transition states. A thorough conformational search was performed in the transition state region to locate the most stable transition state in both H-ZSM-5 and H-beta, such that a lower limit of the reaction barrier in each catalyst is obtained. The transition states were subsequently linked to reactant and product complexes using the quasi-IRC approach, in which slight perturbations of the TS along the imaginary frequency are applied to yield initial structures for the optimization toward reactants and products.

Energies of the final stationary points were further refined by single-point calculations at the B3LYP-D [37-39] and ωB97X-D [40] levels of theory, which include dispersion interactions. All energy calculations were performed using the 6-31+G(d) basis set, which was previously found to be sufficiently large; extension toward a triple-zeta basis set had only a minor effect on the resulting interaction energies and barriers [20]. In the B3LYP-D approach, dispersion corrections as proposed by Grimme are added to the standard B3LYP-energy [39]. The ωB97X-D functional is a recently developed long-range corrected functional, in which dispersion is also accounted for by pairwise potential terms. In contrast to Grimme's approach, however, all parameters in the functional form were determined simultaneously [40]. A benchmarking study

by Goerigk and Grimme found the ωB97X-D functional to be a promising method for main group thermochemistry and kinetics, as well as non-covalent interactions [41]. In a recent article this functional was found to perform very well for the adsorption of various guest molecules at the Brønsted sites inside the pores of H-ZSM-5 [30].

All calculations were performed using the Gaussian03 [42] and Gaussian09 [43] packages. Dispersion corrections to the B3LYP energies were calculated using the dftd3-program available from Grimme's group [44]. The cluster models were constructed using ZEOBUILDER [45, 46].

The PHVA-method, implemented in the TAMKIN-toolkit [46, 47], was used to exclude the terminating hydrogens with constrained positions from the normal mode analysis. Partition functions were calculated in the temperature range 250 - 400 °C. Rate constants were determined from the transition state theory (TST). More details are given in Section 3.3.

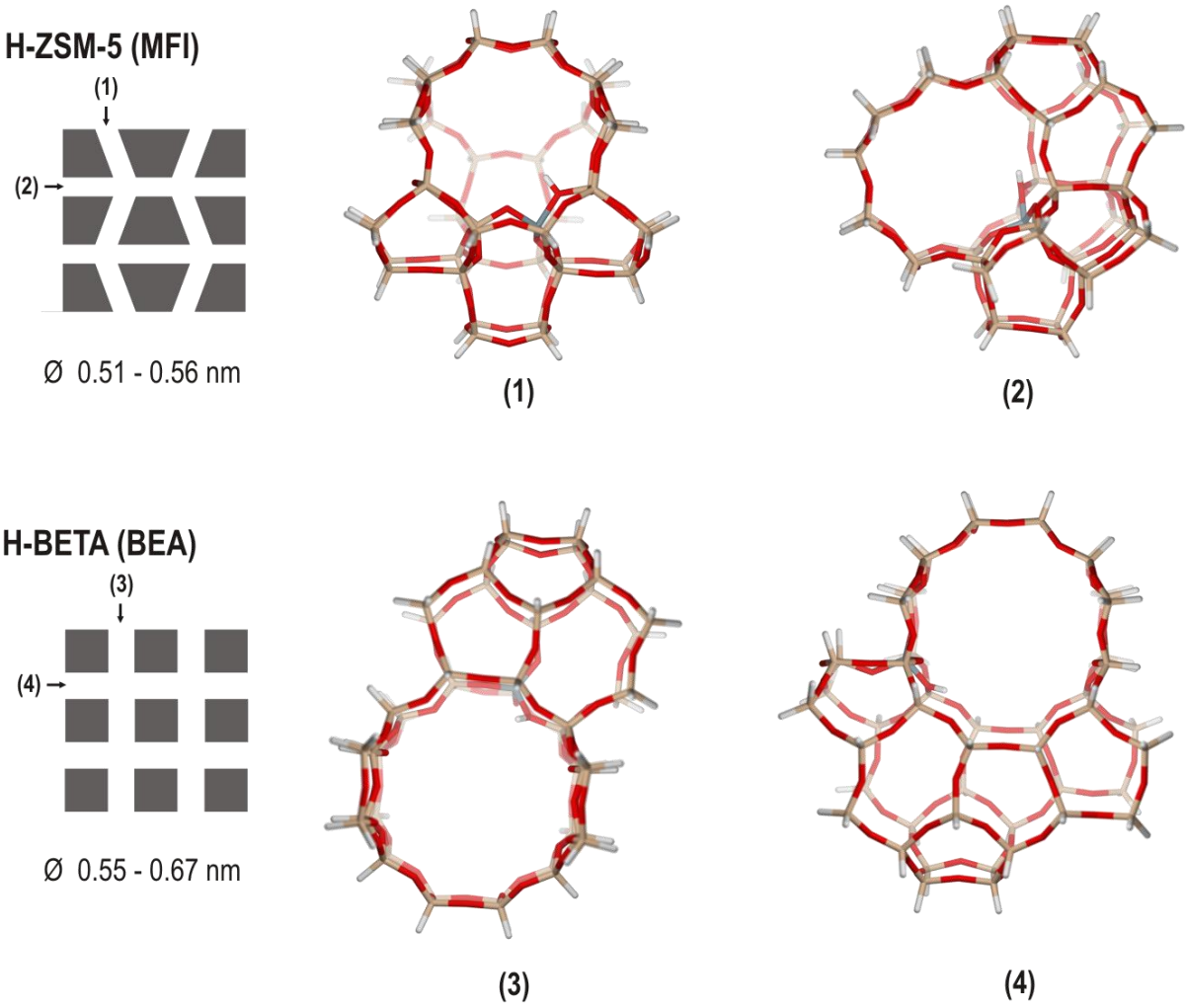

Figure 2. Cluster models used to represent the zeolite catalysts. A single Brønsted acid site is located at the channel intersection. The H-ZSM-5 model (top) contains 46 T-atoms, the H-beta model (bottom) contains 52 T-atoms.

3. RESULTS AND DISCUSSION

3.1. CATALYST CHARACTERIZATION

For the sake of brevity, the primary characteristics of the H-ZSM-5 and H-beta catalysts are summarized in Table 1. XRD confirmed the high crystallinity of both catalysts. The BET surface areas are fairly high for these topologies, also indicative of high-quality materials of good crystallinity. Both catalyst samples comprise similarly sized small primary crystallites, which will reduce effects of diffusion limitations and prevent rapid deactivation. The ^{27}Al MAS-NMR spectra of both catalysts (not shown) displayed only one fairly sharp peak centered at ~50 ppm, the expected chemical shift for Al in a tetrahedral environment. No signal was discernible at ~0 ppm, where octahedral Al will give rise to intensity. Thus, Al is almost exclusively present in tetrahedral framework positions in the zeolites. FT-IR confirmed that all acid sites were accessible to the CO probe molecules, as the peaks assigned to the ν(OH) mode of the Brønsted sites were completely eroded. The magnitudes of the shifts in the ν(OH) vibrational frequencies of the Brønsted sites upon perturbation by adsorbed CO are listed in Table 1. These values constitute a convenient measure of the acid strength of the catalysts and are very similar to previously reported values for H-ZSM-5 and H-beta [48, 49], thus confirming the presence of strong Brønsted acidity and that the catalysts employed here are representative for the respective topologies. Elemental analysis by ICP-MS indicates very similar Si/Al ratios, and this is confirmed by NH_3-TPD. The slight underestimation of Al from NH_3-TPD may suggest that some of the acid sites are inaccessible. Also, it should be kept in mind that the probe molecules employed (CO and NH_3) are somewhat smaller than the methanol-benzene methylation complex. Nevertheless, it appears that there is no significant difference in the density of

Brønsted acid sites between the two catalysts, meaning that the experimentally measured rates can directly be compared.

Table 1. Characteristic data for the two catalysts.

catalyst	**particle size (SEM/TEM)**	**Si/Al ratio (ICP-MS)**	**Si/Al ratio (NH_3-TPD)**	**BET surface area**	**$\Delta\nu(OH)_{Brønsted}$ (CO adsorption)**
H-ZSM-5	~50 nm	45	57	409 m^2/g	-347 cm^{-1}
H-beta	~100 nm	44	61	630 m^2/g	-341 cm^{-1}

3.2. KINETIC MEASUREMENTS OF BENZENE METHYLATION

^{12}C benzene (17 mbar) and ^{13}C methanol (37 mbar) were co-reacted over the H-ZSM-5 and H-beta catalysts described above at 350 °C. The CT was varied between 0.0038 and 0.0096 h by adjusting the total gas flow through the reactor. The conversion of the feed mixture (determined by considering benzene, methanol, and dimethyl ether to be unconverted reactants) and the rate of conversion (the product of the fractional conversion and the WHSV) are shown in Figure 3 below. The most striking feature of Figure 3 is the higher activity of H-ZSM-5 compared with H-beta. This is a primary finding of this investigation and the origin of this difference will be elaborated below.

As expected, the conversion (Figure 3, left panel) increases with increasing CT. It should be noted that, in particular at the shortest CTs, the conversion is sufficiently low to reasonably assume differential conditions, which considerably simplifies the kinetic analysis. For both

catalysts, the rate of conversion increases with increasing CT. This is related to the well-known autocatalytic nature of the conversion of methanol to hydrocarbons [5, 50, 51]. Linear extrapolation of the rate of conversion to CT = 0 gives a limiting rate of conversion of 9.9 and 2.6 $g_{feed\ converted}\ g_{catalyst}^{-1}\ h^{-1}$ for H-ZSM-5 and H-beta, respectively.

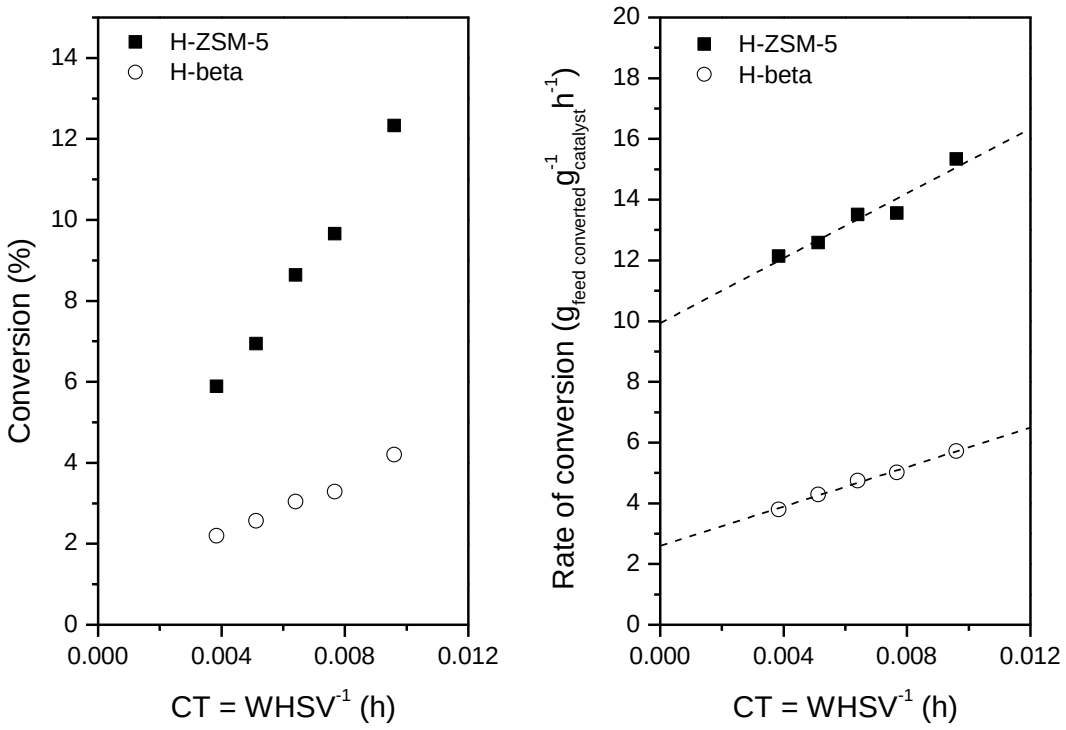

Figure 3. Conversion of feed mixture (left panel) and rate of conversion (right panel) measured as a function of contact time (CT) for the co-reaction of benzene and methanol over H-ZSM-5 and H-beta. 17 mbar of benzene and 37 mbar of methanol were co-reacted at 350 °C. The CT was varied between 0.0038 and 0.0096 h by adjusting the total gas flow through the reactor. The dashed lines are linear fits.

Product selectivities are presented in Figure 4. Clearly, for both catalysts, toluene, which is the primary methylation product, dominates strongly displaying a selectivity between 65 and 75 %. The toluene selectivity decreases with increasing CT, as secondary reactions leading to other products become more prominent. Extrapolation of the toluene selectivity to CT = 0 gives a primary selectivity close to 80 % for both catalysts. Isotopic analysis of the toluene showed that close to 95 % of the toluene molecules contained only one ^{13}C atom, as expected for toluene formation via methylation of ^{12}C benzene by ^{13}C methanol. Analysis revealed no significant variations of the isotopic distribution over the investigated range of CTs. Thus, it can safely be assumed that direct toluene formation from methanol is negligible in these experiments. Product and isotopic selectivities apparently do not extrapolate to unity, implying that reactions other than methylation will occur even at infinitesimal conversions. Possible causes of this observation have been discussed previously [17].

Notably, the second most abundant product is not the same for the two catalysts. For H-ZSM-5 (Figure 4, left panel), the xylenes are in clear excess compared with the other secondary products. In stark contrast, for H-beta, hexamethylbenzene is the most prominent by-product. Additionally, for both catalysts, minor amounts of C_9-C_{11} methylbenzenes and aliphatics are formed. The isotopic composition of the minor products was not determined. However, it appears likely that for H-ZSM-5, the xylenes and the other byproducts detected in effluent are formed via double methylations and hydrocarbon pool type reactions, respectively. Hexamethylbenzene is known to be a major product in MTH and alkylation reactions over large-pore H-beta, in contrast to what has been observed for medium-pore H-ZSM-5 [52]. The low abundance of C_9-C_{11} methylbenzenes relative to hexamethylbenzene might suggest that the MTH reaction is suppressed to a somewhat lesser extent in H-beta compared with H-ZSM-5, even in these experiments carried out at extremely high feed rates. For both catalysts, the

formation of side products will lead to a minor underestimation of the methylation rates, as methylation products are consumed in further reactions, and acid sites are involved in other reactions than methylation. The purpose of the extrapolation procedure described above is to minimize these effects.

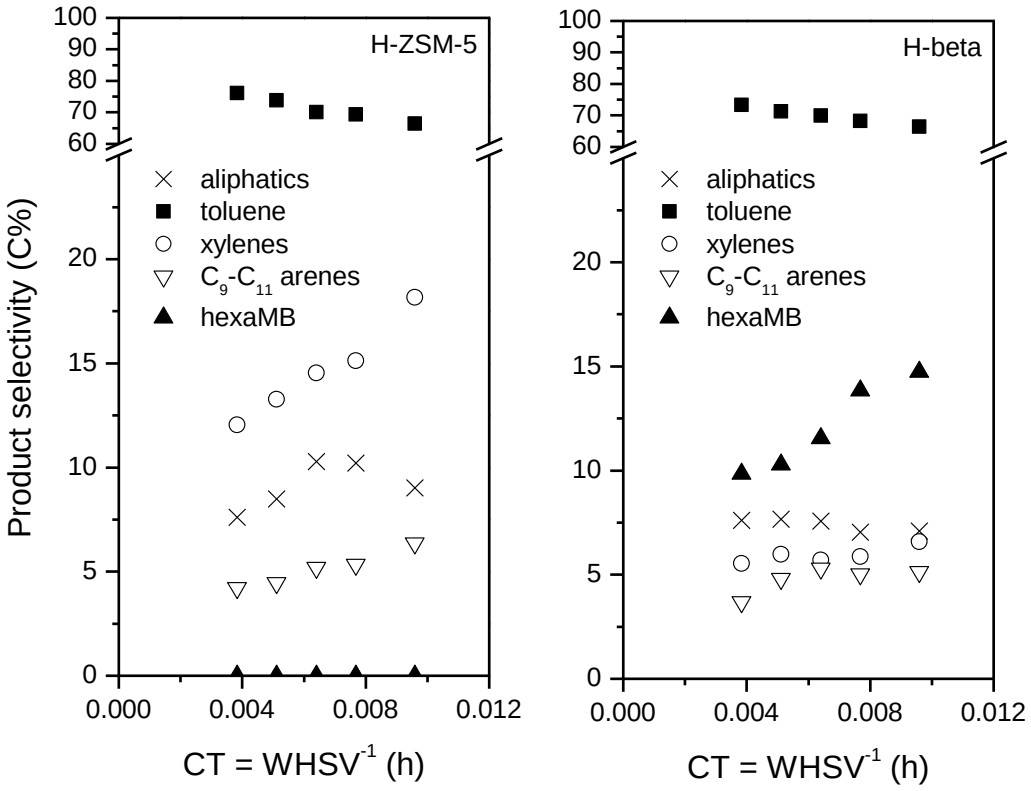

Figure 4. Product selectivities for H-ZSM-5 (left panel) and H-beta (right panel) measured as a function of contact time (CT) for the co-reaction of benzene and methanol over H-ZSM-5 and H-beta. 17 mbar of benzene and 37 mbar of methanol were co-reacted at 350 °C. The CT was varied between 0.0038 and 0.0096 h by adjusting the total gas flow through the reactor (hexaMB = hexamethylbenzene).

The reaction orders with respect to benzene and methanol were determined by individually varying the partial pressure of each reactant while keeping that of the other constant. These experiments were carried out with constant total gas flow through the reactor at 350 °C. As is clearly seen in Figure 5, the higher methylation activity of H-ZSM-5 relative to H-beta is maintained over an extended range of conditions. In agreement with previous reports for the methylation of alkenes [17, 18, 22], the reaction orders are one for benzene and very close to zero for methanol, resulting in the following empirical rate law:

$$r = k\, p^{0}_{\text{methanol}}\, p^{1}_{\text{benzene}}$$

The interpretation of the reaction orders is that the zeolite acid sites are fully covered by the methylating species and benzene is scarcely adsorbed at these conditions. Several quantum chemical studies have shown that methanol is likely to be strongly adsorbed on the Brønsted acid sites, whereas the species being methylated is loosely adsorbed in the close vicinity [19-21]. This was also confirmed by the theoretical simulations of the benzene methylation reaction carried out in the current study (cf. infra).

The reaction temperature was varied in order to determine the apparent activation energy for the methylation of benzene over the two catalysts. The Arrhenius plots shown in Figure 6 display the expected linear behavior. The apparent activation energy was determined to be 58 and 56 kJ mol^{-1} for H-ZSM-5 and H-beta, respectively. As a consequence of the reaction orders as described above, this apparent activation energy is the sum of the intrinsic activation energy and the benzene adsorption energy, which is a negative number (see also Figure 1):

$$\Delta E^{\ddagger}_{\text{app}} = \Delta E^{\ddagger}_{\text{int}} + \Delta E_{\text{ads,benzene}}$$

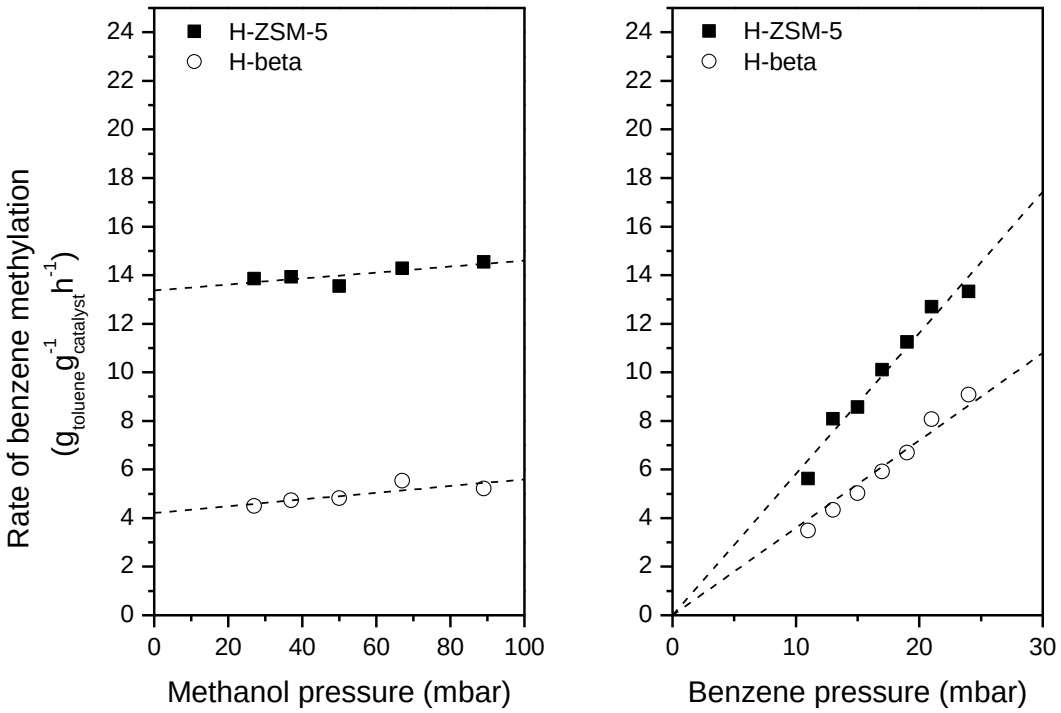

Figure 5. Rate of methylation, derived from the yield of toluene containing only one ^{13}C, for the co-reaction of benzene and methanol over H-ZSM-5 and H-beta as a function of the partial pressures at 350 °C and constant total gas flow = 75 $mLmin^{-1}$. Left panel: 17 mbar of benzene was co-reacted with 27-89 mbar of methanol, CT ranging from 0.0024-0.011 h. Right panel: 11-24 mbar of benzene was co-reacted with 37 mbar of methanol, CT ranging from 0.0042-0.0063 h. The dashed lines are linear fits; these were forced through the origin in the right panel.

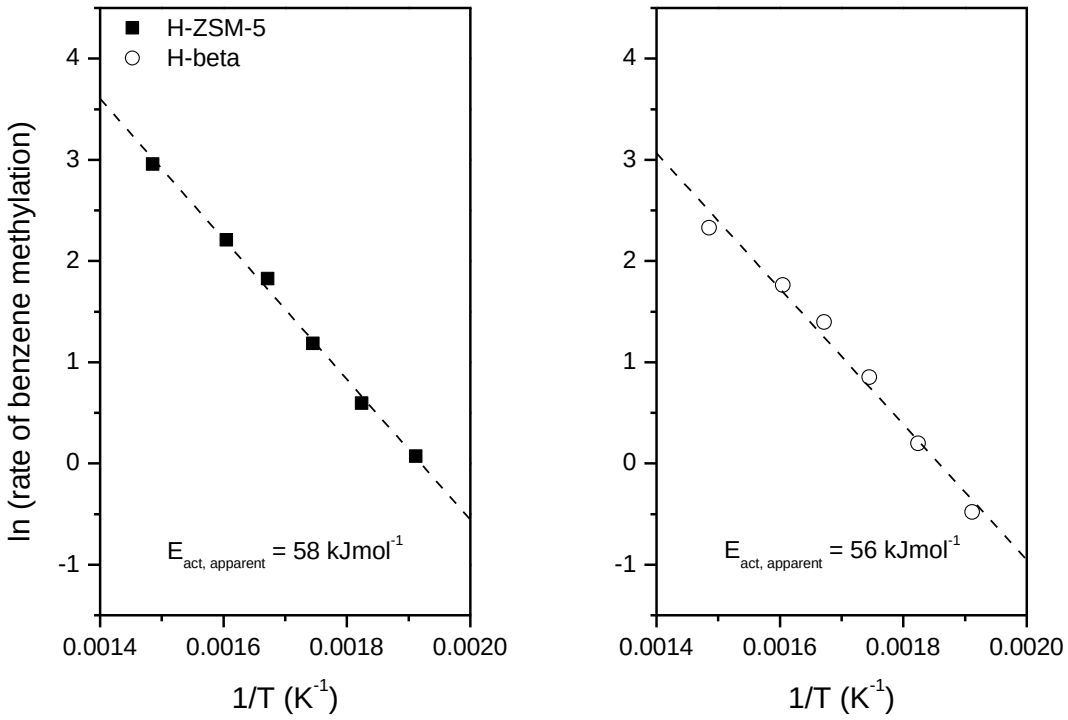

Figure 6. Rate of methylation, derived from the yield of toluene containing only one ^{13}C, for the co-reaction of benzene (17 mbar) and methanol (37 mbar) over H-ZSM-5 (left panel) and H-beta (right panel) as a function of the reaction temperature at constant total gas flow = 75 $mLmin^{-1}$. The temperature was varied between 250-400 °C and CT = 0.0051 h. The dashed lines are linear fits.

The rate constants for benzene methylation over the two catalysts may be calculated from the extrapolated rates of conversion of 9.9 and 2.6 $g_{feed\ converted}\ g_{catalyst}^{-1}\ h^{-1}$ for H-ZSM-5 and H-beta extracted from Figure 3. To facilitate comparison with previous measurements carried out for the methylation of alkenes, the rate constants will be expressed in two sets of units. First, multiplication by the limiting fractional product and isotopic selectivities, which were found to

be 0.8 and 0.95, respectively, for both catalysts, gives the rate of formation of the clean methylation product. Furthermore, the rate constant is conveniently normalized with respect to the benzene pressure, as the rate of methylation is first order with respect to benzene partial pressure. These rate constants can also be expressed with respect to the number of moles of methylation product rather than in grams of toluene. Application of these conversions gives the rate constants listed in the second column of Table 2 for the methylation of benzene over the two catalysts in units of $mol_{toluene}\ g_{catalyst}^{-1}\ h^{-1}\ mbar_{benzene}^{-1}$. Additionally, Table 2 lists pre-exponentials and a selection of previously published values for the methylation of alkenes over the same H-ZSM-5 catalyst as employed here.

Table 2. Experimental kinetic parameters for the methylation of benzene. Data for the methylation of alkenes are taken from [17, 18].

	k (350 °C)	**A**	**E_a**
	mol g^{-1} h^{-1} $mbar^{-1}$	mol g^{-1} h^{-1} $mbar^{-1}$	kJ mol^{-1}
benzene/H-ZSM-5	4.8×10^{-3}	3.3×10^{2}	58
benzene/H-beta	1.3×10^{-3}	5.8×10^{1}	56
ethene/H-ZSM-5	2.4×10^{-4}	1.2×10^{5}	103-114
propene/H-ZSM-5	4.5×10^{-3}	2.0×10^{3}	69
n-butene/H-ZSM-5	1.3×10^{-2}	7.7×10^{1}	45

As emphasized above, the rate constants clearly show that H-ZSM-5 is a more active methylation catalyst than H-beta. For H-ZSM-5, the rate of benzene methylation appears to be comparable with the rate of propene methylation.

A discussion of the possible uncertainties associated with these experimental kinetic parameters is required. The linear regression analysis yields standard deviations close to 3 kJ mol^{-1} for the barriers, but it should be underlined that this constitutes a significant underestimation of the actual uncertainty in these experiments. Clearly, systematic and random errors in the experiments related to the measurements of reaction temperature, gas flows, and catalyst mass are non-negligible. The above analysis presupposes strict adherence to Arrhenius behavior and unchanging reaction orders in the investigated temperature range. Previously, we have assigned the uncertainty in the barriers to be at least ± 5 kJ mol^{-1} [19]. This uncertainty arises primarily from the cumulative uncertainties in the reactor setup and deviations from strict Arrhenius behavior. As the experimentally determined quantity is the rate constant, which comprises both the pre-exponential and the exponential Arrhenius factor, these will have equal uncertainty; ± 5 kJ mol^{-1} in the exponential factor corresponds to about one order of magnitude in the pre-exponential.

In the following paragraphs, the same methylation reactions will be modeled using quantum chemical methods; it is thus relevant to consider the extent to which the two approaches are comparable. Firstly, as mentioned in the introduction, we have assumed that methylation occurs in a concerted rather than stepwise manner, both in the interpretation of the experimental measurements and in the theoretical description. Secondly, while the formation of by-products cannot be completely avoided when operating at realistic reaction temperatures, by-product formation is not readily accounted for using theoretical methods. Indeed, the main strength of

these methods is their ability to isolate single reaction steps. As previous spectroscopic investigations have indicated that byproducts such as hexamethylbenzene might block a fraction of the available acid sites, experimental measurements could underestimate the initial the methylation activity of the catalyst described by the theoretical simulations [28].

3.3. COMPUTATIONAL STUDIES OF BENZENE METHYLATION

A systematic first-principles study was performed to calculate reaction rates for benzene methylation in both H-ZSM-5 and H-beta, such that they are directly comparable with the experimentally measured ones (Section 3.2). Within this set of simulations, the various factors contributing to barriers and pre-exponential factors can be separated, leading to a more profound understanding of the observed differences between the two catalysts.

As shown in a previous paper by some of the authors, zeolite-catalyzed methylation reactions can be modeled in either a unimolecular or a bimolecular fashion [20]. In the unimolecular approach, all reactants are considered to have formed a pre-activated complex at the zeolite active site. This complex can henceforth be treated as a single molecule undergoing internal rearrangements. The resulting reaction rates are referred to as “intrinsic reaction rates”, which are useful for mutual comparison between competing elementary reactions within the same reaction network, but cannot directly be compared with experimental measurements. In contrast, in the bimolecular approach only methanol is considered already adsorbed at the active site, while benzene is supplied from the gas phase. The latter can be linked conceptually with the experimentally observed reaction orders (zeroth order in methanol, first order in benzene) and results in “apparent reaction rates”, which can be subjected to direct comparison with

experimental results. Likewise, the electronic barriers for the unimolecular and bimolecular reactions are referred to as “intrinsic” and “apparent” barriers, respectively.

The electronic energy differences corresponding to the consecutive steps in the energy profile for benzene methylation (Figure 1) are summarized in Table 3 and will each be discussed in more detail in the following paragraphs.

Table 3. Electronic energy differences in kJ mol^{-1} corresponding to the different steps in the energy diagram, given at different levels of theory.

	H-ZSM-5			**H-beta**		
	B3LYP	B3LYP-D3	ωB97X-D	B3LYP	B3LYP-D3	ωB97X-D
$\Delta E_{ads,methanol}$	-75	-117[a]	-108	-89	-120	-111
$\Delta E_{ads,benzene}$	-14	-106	-92	-3	-65	-56
$\Delta E^{\ddagger}_{int}$	120	112	131	117	98	118
$\Delta E^{\ddagger}_{app}$	106	5	39	114	33	62

[a]Value differs from the one reported in ref. [20] due to different position of the zeolite proton. In the current paper, adsorption is always considered at the Brønsted site found by following the IRC from the TS.

3.3.1. METHANOL ADSORPTION

The first step in the methylation of benzene consists of the adsorption of methanol at the Brønsted acid site (Figure 1) through the formation of two hydrogen bonds. At the B3LYP-level, the adsorption energy is about 14 kJ mol^{-1} higher in H-beta, which could be related to the differences in hydrogen bonding between the two catalysts (see Figure 7). While the primary hydrogen bond, between the methanol oxygen and the zeolite proton, is almost identical in length in both cases (1.48 Å in H-ZSM-5 vs. 1.49 Å in H-beta), the secondary hydrogen bond, between the methanol proton and a framework oxygen, is slightly longer in H-beta (2.14 Å) than in H-ZSM-5 (1.85 Å). The secondary hydrogen bond in H-ZSM-5 is formed with a nearest-neighbor framework oxygen, as opposed to a next-nearest-neighbor oxygen in H-beta. When dispersion interactions are taken into account (B3LYP-D3 and ωB97X-D), the energy of methanol adsorption is very similar in H-ZSM-5 and H-beta. For H-ZSM-5, these theoretical estimates may be compared to the experimental results reported by Lee et al. These authors have measured differential heats of adsorption at 400 K for a series of alcohols and nitriles in H-ZSM-5 and silicalite, and obtained an adsorption enthalpy -115 ± 5 kJ mol^{-1} for methanol on H-ZSM-5, which agrees very well with our theoretical results at the B3LYP-D3 or ωB97X-D levels. Nevertheless, it should be noted that the theoretical values in Table 3 are purely electron energy differences, which are only comparable with the experimental adsorption enthalpy after appropriate thermal corrections are included. Recently, the adsorption of alcohols and nitriles in H-ZSM-5 was studied in more detail, using the methodology employed in the current article. The thermal correction to the adsorption enthalpy at 400 K was shown to amount to about 6 kJ mol^{-1} for all adsorbates considered [30].

3.3.2. BENZENE CO-ADSORPTION AND METHYLATION

In the ensuing steps, benzene is co-adsorbed onto the methanol complex and subsequently methylated in a one-step (concerted) mechanism. The transition states are very similar in both catalysts (see Figure 7), even though more space is available in H-beta: the length of the C-C bond being formed is 2.14 Å in H-ZSM-5 and 2.06 Å in H-beta, the length of the C-O bond being broken is 2.22 Å in H-ZSM-5 and 2.23 Å H-beta.

The accuracy of the apparent barrier to methylation will depend on the accuracy of both the benzene co-adsorption energy and the intrinsic barrier. As mentioned in the Methodology section, a thorough examination of all possible active sites and adsorption modes is beyond the scope of this study. To ensure an unambiguous definition in both catalysts under comparison, the co-adsorption energy is consistently calculated by removing the benzene molecule from the pre-transition state reactants and optimizing the resulting methanol complex. This approach avoids non-reproducible errors resulting from unintentional deformations of the zeolite framework.

Due to the smaller available space in H-ZSM-5, the adsorbed methanol shifts slightly upon co-adsorption of a benzene molecule, resulting in a less optimal hydrogen-bonded configuration, which corresponds to a destabilization of about 10 kJ mol^{-1} (at the B3LYP-level). Using the standard B3LYP-functional, the final co-adsorption energy amounts to only -14 kJ mol^{-1} in H-ZSM-5, and an almost negligible -3 kJ mol^{-1} in H-beta (Table 3). In experimental studies comparing benzene adsorption on H-ZSM-5 and silicalite, very similar gravimetrical uptakes and heats of adsorption were reported for both materials, indicating that the stabilization of benzene within the zeolite pores is mainly due to dispersive interactions with the pore walls

[53]. Standard DFT-functionals are unable to account for these van der Waals interactions, which are clearly crucial to describe the actual stabilization. When adding Grimme-dispersion corrections to the B3LYP energies, the co-adsorption energy increases to -106 and -65 kJ mol^{-1} in H-ZSM-5 and H-beta, respectively. The co-adsorption energy is larger in H-ZSM-5 due to a tighter fit of the guest molecules in the zeolite pores; in H-beta more empty space remains upon co-adsorption of benzene and methanol at the active site (see Figure 7). (To quantify this difference in available space, note that the maximum diameter of a sphere that can be included in the zeolite framework is 6.3 Å in MFI, compared to 6.62 Å in BEA.[31])

Evidently, the magnitude of the dispersive interactions is immediately related to the size of the adsorbed species, and much larger D-corrections are expected for the co-adsorption of benzene, compared to the smaller alkenes studied in a previous paper. A closer look at the actual values of the interaction energy before and after applying the correction reveals, however, that for benzene the calculated co-adsorption energy is entirely dominated by the (empirical) correction terms.

If we apply the Grimme dispersion corrections to the intrinsic B3LYP barriers, the latter drop from 120 to 112 kJ mol^{-1} in H-ZSM-5 and from 117 to 98 kJ mol^{-1} in H-beta. However, adding the dispersion-corrected benzene co-adsorption energies to the corresponding intrinsic barriers results in apparent barriers at the B3LYP-D level which are clearly unrealistically low (5 and 33 kJ mol^{-1}), in particular when compared to the experimental data. In an effort to improve these results, we re-calculated the electronic energies with the recent ωB97X-D functional. In this long-range-corrected functional dispersion is included in a similar fashion to Grimme's approach, but all parameters have been fitted simultaneously. This functional was shown to perform somewhat better than classic dispersion-corrected functionals for various properties, including atomization and reaction energies [40, 41]. At the ωB97X-D level of theory, the

benzene co-adsorption energies in H-ZSM-5 and H-beta are only slightly smaller than the B3LYP-D values, -92 and -56 kJ mol^{-1} respectively. However, the intrinsic barriers predicted by ωB97X-D are almost 20 kJ mol^{-1} higher (131 and 118 kJ mol^{-1} for H-ZSM-5 and H-beta). As a result, the final apparent barriers are 39 and 62 kJ mol^{-1}, which is closer to the experimentally expected values. Note that the values mentioned in this section are purely electronic energies. As thermal corrections are generally small compared with the electronic energy differences, the latter are, however, sufficient to assess which density functional is best suited for describing methylation barriers and kinetics (cf. infra).

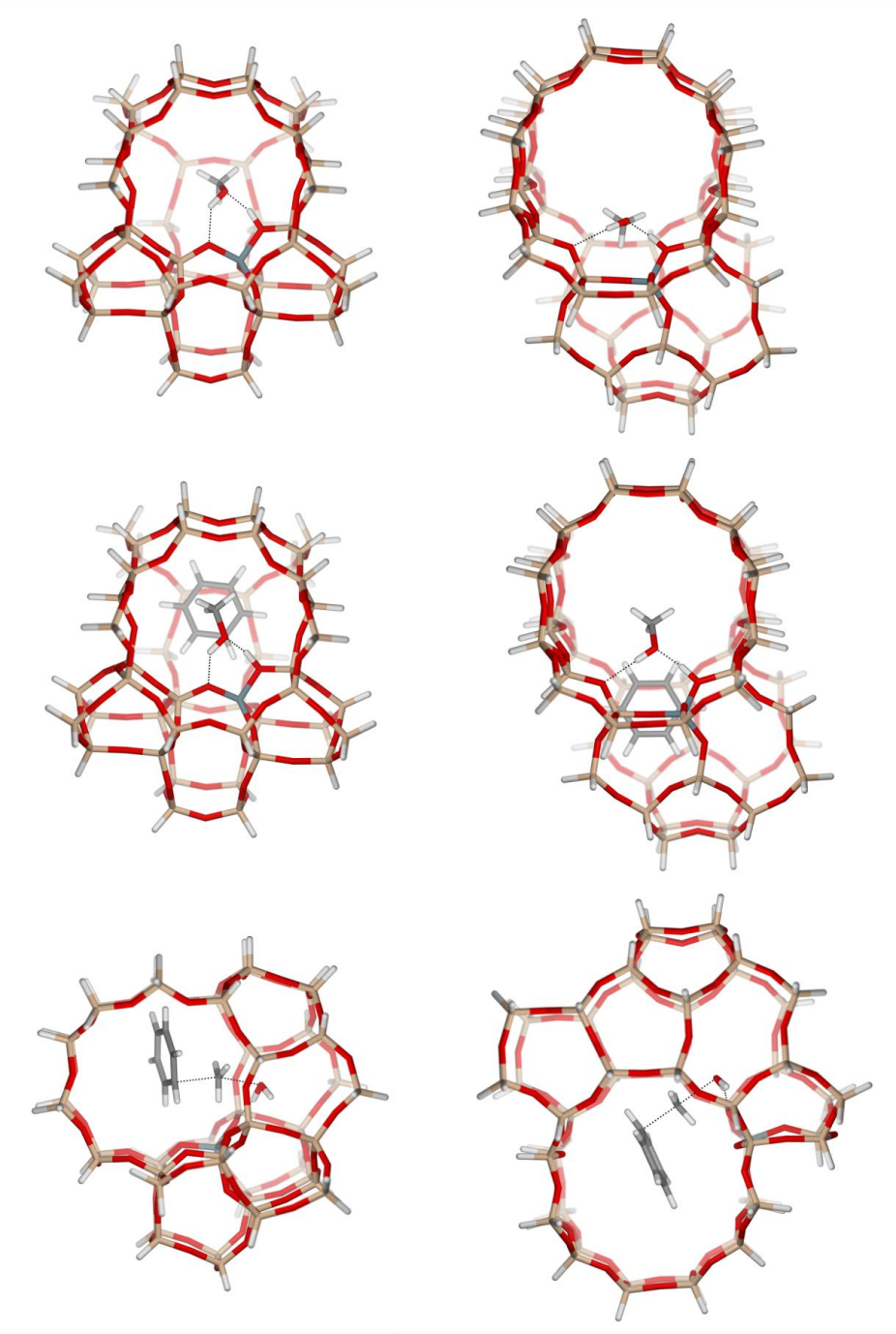

Figure 7. From top to bottom: adsorbed methanol, pre-TS reactant complex and transition state for benzene methylation in H-ZSM-5 (left) and H-beta (right).

3.3.3. RATE CONSTANTS AND KINETIC PARAMETERS

A primary objective of this contribution is to directly compare rates of reaction, rather than comparing Arrhenius barriers to electronic energies. To this end, both intrinsic and apparent methylation kinetics are calculated using transition state theory. Intrinsic rate constants result from considering the methylation as a unimolecular rearrangement of the reactant complex:

$$k_{uni} = \frac{k_B T}{h} \frac{q^{\ddagger}_{TS}}{q_{Z\text{-}H,\ MeOH(ads),\ \ benzene\ \ (ads)}} \exp\left(\frac{-\Delta E^{\ddagger}_{int}}{RT}\right)$$

A bimolecular approach yields apparent rate constants:

$$k_{bi} = \frac{k_B T}{h} \frac{q^{\ddagger}_{TS}}{q_{Z\text{-}H,\ MeOH(ads)}\ q_{\ benzene\ \ (g)}} \exp\left(\frac{-\Delta E^{\ddagger}_{app}}{RT}\right)$$

k_B, h and R are the Boltzmann, Planck and universal gas constants; q_X are the partition functions of species X. Partition functions and rate constants are calculated in the temperature range 250 - 400 °C (consistent with the experimental temperature range), after which the kinetic parameters are determined from fitting rate constants to the Arrhenius equation. Activation energies (E_a), pre-exponential factors (A) and rate constants at 350 °C are summarized in Table 4. To allow comparison with the previously studied methylations of small alkenes in H-ZSM-5 [20], the electronic energies for those reactions are also evaluated at the ωB97X-D/6-31+g(d)-level, and rate constants and Arrhenius parameters are re-calculated with the methodology used for the benzene methylation. In agreement with the experimental results (see Section 3.2), the rate of benzene methylation seems to be similar to the rate of propene methylation.

Table 4. Arrhenius parameters and rate constants at 350 °C for methylation reactions in H-ZSM-5 and H-beta. Electronic energies were evaluated at the ωB97X-D/6-31+g(d)-level.

	unimolecular			*bimolecular*		
	A	**E_a**	**k(350 °C)**	**A**	**E_a**	**k(350 °C)**
	1/s	kJ mol^{-1}	1/s	m^3/mol/s	kJ mol^{-1}	m^3/mol/s
benzene/ H-ZSM-5	1.9×10^{12}	131	1.8×10^{1}	1.6×10^{4}	56	3.0×10^{-1}
benzene/ H-beta	5.5×10^{10}	120	5.1×10^{0}	1.2×10^{5}	79	2.7×10^{-2}
ethene/ H-ZSM-5[a]	1.0×10^{11}	104	2.0×10^{2}	1.2×10^{6}	91	2.7×10^{-2}
propene/ H-ZSM-5 [a]	6.0×10^{11}	99	3.3×10^{3}	5.8×10^{4}	64	2.6×10^{-1}
t-2-butene/ H-ZSM-5 [a]	5.9×10^{11}	97	4.1×10^{3}	8.5×10^{3}	45	1.3×10^{0}

[a] Previously reported in ref. [20]. Kinetic parameters were re-calculated to be fully consistent with the methodology used in the current paper.

Both the unimolecular and bimolecular kinetic data show that benzene methylation is faster in H-ZSM-5 compared to H-beta, in agreement with the experimental results. In H-beta, more space is available, such that the entropy loss upon reaction is smaller compared with H-ZSM-5, which should result in a larger pre-exponential factor. This behavior is only retrieved using the

bimolecular approach, as the largest entropy loss will naturally occur during the co-adsorption of benzene, which is not taken into account in the unimolecular model.

To validate this observation, enthalpy, entropy, and free energy differences at 350 °C were calculated for the steps following methanol adsorption, based on electronic energies at the ωB97X-D/6-31+g(d)-level. The resulting energy profiles are plotted in Figure 8. For the unimolecular reaction, the intrinsic enthalpy barrier ($\Delta H^{\ddagger}_{int}$) at 350 °C is actually higher in H-ZSM-5 (127 vs. 115 kJ mol^{-1}), but the entropy loss ($T\Delta S^{\ddagger}_{int}$) upon reaction is smaller, amounting to -15 kJ mol^{-1} in H-ZSM-5 and -33 kJ mol^{-1} in H-beta, such that the final intrinsic free energy barrier ($\Delta G^{\ddagger}_{int}$) is only slightly smaller in H-ZSM-5 compared to H-beta (142 vs. 148 kJ mol^{-1}). If we consider the bimolecular model, the apparent free energy barrier ($\Delta G^{\ddagger}_{app}$) is 13 kJ mol^{-1} smaller in H-ZSM-5 than in H-beta (147 vs. 160 kJ mol^{-1}), resulting in a significantly higher methylation rate in H-ZSM-5, even though the contribution due to entropy loss is larger ($T\Delta S^{\ddagger}_{app}$ = -100 vs. -90 kJ mol^{-1}). These values show that the observed difference in methylation rate between the two catalysts is ultimately due to differences in the benzene co-adsorption step. Co-adsorption of benzene and methanol is energetically favored in the medium-sized pores of H-ZSM-5 ($\Delta H_{ads,benzene}$ = -80 vs. -45 kJ mol^{-1}), to the extent that the stronger interactions of the guest molecules with the active site and the zeolite walls eventually outweigh the higher entropy loss ($T\Delta S_{ads,benzene}$ = -85 vs. -57 kJ mol^{-1}).

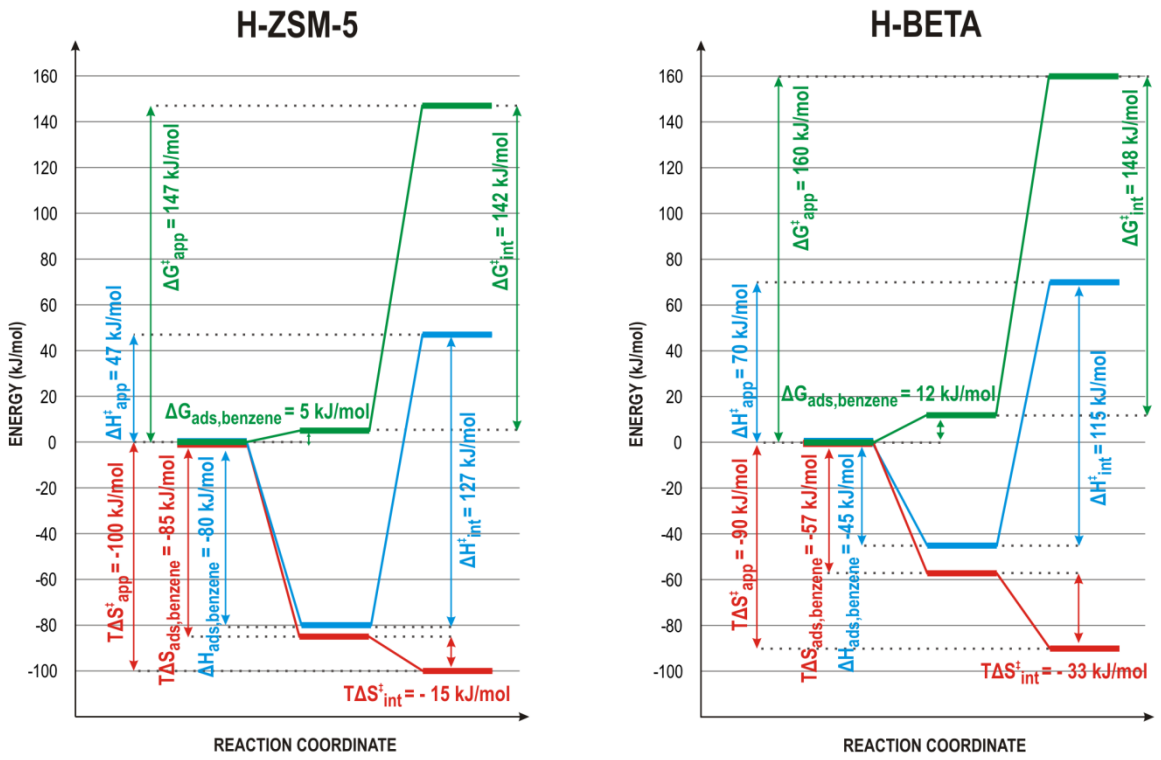

Figure 8. Enthalpic, entropic and total free energy profile for benzene methylation in H-ZSM-5 and H-beta at 350 °C, starting from adsorbed methanol. (LOT electronic energy: ωB97X-D/6-31+g(d)).

To enable a direct comparison between theoretical and experimental values, the (bimolecular) theoretical rate coefficients are normalized per mbar of benzene partial pressure and per g catalyst, by taking into account the number of active sites per g catalyst as inferred from NH_3-TPD (see Section 2.1) for both catalyst samples. The resulting rate constants in mol $g^{-1}h^{-1}mbar^{-1}$ are listed together with the experimental values in Table 5. In general, the theoretical rate constants correspond very well with the experimental values and show that benzene methylation is considerably faster in H-ZSM-5 compared with H-beta, although the theoretical results predict an even larger difference between the two catalysts. Additionally, the theoretical activation

energy is larger in H-beta than in H-ZSM-5 (74 vs. 51 kJ mol^{-1}), in contrast to the experimental values, which were found to be rather similar for both zeolites (56 vs. 58 kJ mol^{-1}). The separate kinetic parameters (E_a and A) are prone to larger uncertainties caused by the fitting procedure and choice of temperature interval; it is therefore safer to compare theoretical and experimental rate constants rather than individual Arrhenius parameters.

Table 5. Direct comparison between theoretical and experimental kinetic parameters at 350°C (LOT electronic energy: ωB97X-D/6-31+g(d)).

	theoretical			*experimental*			
	A	**E_a**	**k(350 °C)**	**A**	**E_a**	**k(350 °C)**	$k_{theoy.}/k_{experiment}$
	mol g^{-1} h^{-1} $mbar^{-1}$	kJ mol^{-1}	mol g^{-1} h^{-1} $mbar^{-1}$	mol g^{-1} h^{-1} $mbar^{-1}$	kJ mol^{-1}	mol g^{-1} h^{-1} $mbar^{-1}$	
H-ZSM-5	1.2×10^2	51	6.1×10^{-3}	4.4×10^2	58	5.8×10^{-3}	1.0
H-beta	8.6×10^2	74	5.1×10^{-4}	1.9×10^2	56	3.7×10^{-3}	0.1
$k_{H\text{-}ZSM\text{-}5}/\ k_{H\text{-}beta}$			12.0			1.56	

4. CONCLUSIONS

In this article, the kinetics of benzene methylation by methanol have been investigated over two acidic zeolite catalysts, H-ZSM-5 and H-beta. Experimental measurements were performed in a setup that uses very high feed rates to study the system at low conversion. By adopting this approach, side reactions are suppressed, such that the actual rate of the methylation step can be directly monitored. From these methylation rates, kinetic coefficients, reaction orders, and Arrhenius parameters can be determined. H-ZSM-5 appears to be a more active methylation catalyst than H-beta, showing a consistently higher methylation rate across a range of experimental conditions in which both methanol and benzene partial pressures were varied. The methylation reaction is found to be first order with respect to benzene and zeroth order with respect to methanol. The experimental Arrhenius barriers are similar for the two catalysts. To gain a more profound understanding of the cause of the observed difference in methylation rate between the two catalysts, theoretical simulations have been performed. The methylation reaction was modeled in both H-ZSM-5 and H-beta using modern dispersion-corrected DFT-methods that allow accounting for all relevant interactions between the guest molecules and the zeolite environment. These calculations reproduce the higher rate of methylation over H-ZSM-5 and indicate that this may be attributed to a stronger co-adsorption of benzene in the more narrow H-ZSM-5 pores. Host-guest interactions in the MFI-topology are more favorable and outweigh the greater loss of entropy compared with the more spacious BEA-framework. This difference in entropy loss is also reflected in the pre-exponential factor, which is slightly smaller in H-ZSM-5 than in H-beta.

ACKNOWLEDGEMENTS

This publication forms a part of the inGAP Center of Research-based Innovation, which receives financial support from the Research Council of Norway under contract no. 174893. This work was also supported by the Fund for Scientific Research Flanders (FWO), the Research Board of Ghent University (BOF), and BELSPO in the frame of IAP/6/27. Funding was also received from the European Research Council under the European Community's Seventh Framework Programme [FP7(2007-2013) ERC grant agreement number 240483]. Computational resources (Stevin Supercomputer Infrastructure) and services used in this work were provided by Ghent University, the Hercules Foundation and the Flemish Government – department EWI.

REFERENCES

[1] A. Corma, G. Sastre, P.M. Viruela, J. Mol. Catal. A: Chem. 100 (1995) 75-85.

[2] J. Cobb, New Zealand Synfuel The Story of the World's First Natural Gas to Gasoline Plant, Cobb/Horwood Publication, Auckland, 1985.

[3] H. Koempel, W. Liebner, Stud. Surf. Sci. Catal., Elsevier. 261-267.

[4] J.Q. Chen, A. Bozzano, B. Glover, T. Fuglerud, S. Kvisle, Catal. Today 106 (2005) 103-107.

[5] M. Stöcker, Microporous Mesoporous Mater. 29 (1999) 3-48.

[6] I.M. Dahl, S. Kolboe, J. Catal. 149 (1994) 458-464.

[7] I.M. Dahl, S. Kolboe, Catal. Lett. 20 (1993) 329-336.

[8] I.M. Dahl, S. Kolboe, J. Catal. 161 (1996) 304-309.

[9] J.F. Haw, W. Song, D.M. Marcus, J.B. Nicholas, Acc. Chem. Res. 36 (2003) 317-326.

[10] W.G. Song, D.M. Marcus, H. Fu, J.O. Ehresmann, J.F. Haw, J. Am. Chem. Soc. 124 (2002) 3844-3845.

[11] M. Bjørgen, S. Svelle, F. Joensen, J. Nerlov, S. Kolboe, F. Bonino, L. Palumbo, S. Bordiga, U. Olsbye, J. Catal. 249 (2007) 195-207.

[12] S. Svelle, F. Joensen, J. Nerlov, U. Olsbye, K.P. Lillerud, S. Kolboe, M. Bjørgen, J. Am. Chem. Soc. 128 (2006) 14770-14771.

[13] D. Lesthaeghe, V. Van Speybroeck, G.B. Marin, M. Waroquier, Angew. Chem. Int. Ed. 45 (2006) 1714-1719.

[14] D. Lesthaeghe, B. De Sterck, V. Van Speybroeck, G.B. Marin, M. Waroquier, Angew. Chem. Int. Ed. 46 (2007) 1311-1314.

[15] D. Lesthaeghe, J. Van der Mynsbrugge, M. Vandichel, M. Waroquier, V. Van Speybroeck, ChemCatChem 3 (2011) 208-212.

[16] D.M. McCann, D. Lesthaeghe, P.W. Kletnieks, D.R. Guenther, M.J. Hayman, V. Van Speybroeck, M. Waroquier, J.F. Haw, Angew. Chem. Int. Ed. 47 (2008) 5179-5182.

[17] S. Svelle, P.O. Rønning, S. Kolboe, J. Catal. 224 (2004) 115-123.

[18] S. Svelle, P.O. Rønning, U. Olsbye, S. Kolboe, J. Catal. 234 (2005) 385-400.

[19] S. Svelle, C. Tuma, X. Rozanska, T. Kerber, J. Sauer, J. Am. Chem. Soc. 131 (2009) 816-825.

[20] V. Van Speybroeck, J. Van der Mynsbrugge, M. Vandichel, K. Hemelsoet, D. Lesthaeghe, A. Ghysels, G.B. Marin, M. Waroquier, J. Am. Chem. Soc. 133 (2011) 888-899.

[21] S. Svelle, B. Arstad, S. Kolboe, O. Swang, J. Phys. Chem. B 107 (2003) 9281-9289.

[22] I.M. Hill, S.A. Hashimi, A. Bhan, J. Catal. 285 (2012) 115-123.

[23] M. Bjørgen, U. Olsbye, S. Kolboe, J. Catal. 215 (2003) 30-44.

[24] A. Sassi, M.A. Wildman, H.J. Ahn, P. Prasad, J.B. Nicholas, J.F. Haw, J. Phys. Chem. B 106 (2002) 2294-2303.

[25] A. Sassi, M.A. Wildman, J.F. Haw, J. Phys. Chem. B 106 (2002) 8768-8773.

[26] S. Svelle, M. Visur, U. Olsbye, S. Saepurahman, M. Bjørgen, Top. Catal. 54 (2011) 897-906.

[27] T. Maihom, B. Boekfa, J. Sirijaraensre, T. Nanok, M. Probst, J. Limtrakul, J. Phys. Chem. C 113 (2009) 6654-6662.

[28] S. Saepurahman, M. Visur, U. Olsbye, M. Bjørgen, S. Svelle, Top. Catal. 54 (2011) 1293-1301.

[29] H. Robson, K.P. Lillerud, editors. 2001. Verified Synthesis of Zeolitic Materials. Elsevier Science, Amsterdam.

[30] J. Van der Mynsbrugge, K. Hemelsoet, M. Vandichel, M. Waroquier, V. Van Speybroeck, J. Phys. Chem. C 116 (2012) 5499-5508

[31] Structure Commision of the International Zeolite Association (IZA-SC), Database of Zeolite Structures, http://www.iza-structure.org/databases/.

[32] S. Ban, A. van Laak, P.E. de Jongh, J.P.J.M. van der Eerden, T.J.H. Vlugt, J. Phys. Chem. C 111 (2007) 17241-17248.

[33] H. van Koningsveld, Acta Crystallogr., Sect. B: Struct. Sci. 46 (1990) 731-735.

[34] S. Sklenak, J. Dedecek, C. Li, B. Wichterlova, V. Gabova, M. Sierka, J. Sauer, Phys. Chem. Chem. Phys. 11 (2009) 1237-1247.

[35] S. Sklenak, J. Dedecek, C. Li, B. Wichterlova, V. Gabova, M. Sierka, J. Sauer, Angew. Chem. Int. Ed. 46 (2007) 7286-7289.

[36] J. Dedecek, D. Kaucky, B. Wichterlova, Chem. Commun. (2001) 970-971.

[37] A.D. Becke, J. Chem. Phys. 98 (1993) 5648-5652.

[38] C. Lee, W. Yang, R.G. Parr, Phys. Rev. B 37 (1988) 785.

[39] S. Grimme, J. Antony, S. Ehrlich, H. Krieg, J. Chem. Phys. 132 (2010) 154104.

[40] J.-D. Chai, M. Head-Gordon, Phys. Chem. Chem. Phys. 10 (2008) 6615-6620.

[41] L. Goerigk, S. Grimme, Phys. Chem. Chem. Phys. 13 (2011) 6670-6688.

[42] M.J. Frisch, et al., Gaussian 03 Rev E.01, Gaussian, Inc., Wallingford CT, 2004

[43] M.J. Frisch, et al., Gaussian 09 Rev A.02, Gaussian, Inc., Wallingford CT, 2009

[44] S. Grimme, http://toc.uni-muenster.de/DFTD3/.

[45] T. Verstraelen, V. Van Speybroeck, M. Waroquier, J. Chem. Inf. Model. 48 (2008) 1530-1541.

[46] CMM Code, http://molmod.ugent.be/code/wiki/.

[47] A. Ghysels, T. Verstraelen, K. Hemelsoet, M. Waroquier, V. Van Speybroeck, J. Chem. Inf. Model. 50 (2010) 1736-1750.

[48] M.S. Holm, S. Svelle, F. Joensen, P. Beato, C.H. Christensen, S. Bordiga, M. Bjørgen, Appl. Catal., A 356 (2009) 23-30.

[49] C. Pazé, S. Bordiga, C. Lamberti, M. Salvalaggio, A. Zecchina, G. Bellussi, J. Phys. Chem. B 101 (1997) 4740-4751.

[50] C.D. Chang, Catalysis Reviews-Science and Engineering 25 (1983) 1-118.

[51] C.D. Chang, Shape-Selective Catalysis, American Chemical Society. 96-114.

[52] M. Bjørgen, S. Kolboe, Appl. Catal., A 225 (2002) 285-290.

[53] A. Jentys, G. Warecka, M. Derewinski, J.A. Lercher, J. Phys. Chem. 93 (1989) 4837-4843.